LAWRENCE
LIVERMORE
NATIONAL
LABORATORY

LLNL-SR-492012

Photocathode Optimization for a Dynamic Transmission Electron Microscope: Final Report

P. Ellis, Z. Flom, K. Heinselman, T. Nguyen, S. Tung, R. Haskell, B. W. Reed, T. LaGrange

August 5, 2011

Disclaimer

This work performed under the auspices of the U.S. Department of Energy by Lawrence Livermore National Laboratory under Contract DE-AC52-07NA27344.

PHOTOCATHODE OPTIMIZATION FOR A DYNAMIC TRANSMISSION ELECTRON MICROSCOPE

Final Report

Project Team :
Perry Ellis
Zeke Flom
Karen Heinselman (Fall)
Tim Nguyen
Spencer Tung (Spring)

Project Advisor: Prof. Richard Haskell
Project Liaisons: Drs. Bryan Reed (HMC ’92) and Thomas Lagrange

May 6, 2011

ABSTRACT

The Dynamic Transmission Electron Microscope (DTEM) team at Harvey Mudd College has been sponsored by LLNL to design and build a test setup for optimizing the performance of the DTEM's electron source. Unlike a traditional TEM, the DTEM achieves much faster exposure times by using photoemission from a photocathode to produce electrons for imaging. The DTEM team's work is motivated by the need to improve the coherence and current density of the electron cloud produced by the electron gun in order to increase the image resolution and contrast achievable by DTEM. The photoemission test setup is nearly complete and the team will soon complete baseline tests of electron gun performance. The photoemission laser and high voltage power supply have been repaired; the optics path for relaying the laser to the photocathode has been finalized, assembled, and aligned; the internal setup of the vacuum chamber has been finalized and mostly implemented; and system control, synchronization, and data acquisition has been implemented in LabVIEW. Immediate future work includes determining a consistent alignment procedure to place the laser waist on the photocathode, and taking baseline performance measurements of the tantalum photocathode. Future research will examine the performance of the electron gun as a function of the photoemission laser profile, the photocathode material, and the geometry and voltages of the accelerating and focusing components in the electron gun. This report presents the team's progress and outlines the work that remains.

TABLE OF CONTENTS

1. INTRODUCTION

Lawrence Livermore National Laboratory has sponsored a 2010-2011 Clinic Project to develop a test bed for improving the performance of the photocathode used in their dynamic transmission electron microscope (DTEM). This section introduces LLNL, presents the project statement, and defines the deliverables for the project.

1.1. LLNL AND THE DTEM

Founded in 1952 by the University of California, Lawrence Livermore National Laboratory is a center of cutting-edge research for enhancing national security and continues to fulfill essential roles in national and global security including energy security. The labs were initially founded by the University of California to supplement and compete with Los Alamos National Laboratories in nuclear weapons and radiation research; however, the research conducted at LLNL covers a diverse breadth of topics. The labs boast substantial achievements in fields ranging from computation to fusion energy and from biology to material behavior (Lawrence-Livermore National Laboratory: What We Do).

The DTEM (dynamic transmission electron microscope), winner of R&D100 and Nano50 awards, is a prime example of the unique technical capabilities realized at LLNL. This instrument is the only TEM (transmission electron microscope) in the world capable of capturing high-quality single-shot images of fast-evolving nanostructure and microstructure. What makes the DTEM a unique technical challenge is the high intensity of the electron beam necessary to acquire these high-quality single-shot images (Reed, et. al., “Nanosecond Dynamic...”). LLNL is

sponsoring this project to improve the image quality of the DTEM and next-generation variants. Because of the unique capabilities of this microscope, it is perpetually in high demand for experiments, thus motivating the need for a separate test setup to explore methods for improving image quality without taking the DTEM offline. This is where the Harvey Mudd DTEM clinic team comes in.

1.2. PROJECT STATEMENT

The team will design and build a test bed for investigating the effects of various factors on the quality of the electron beam emitted by a photocathode electron gun. As a stretch goal, the team hopes to examine the beam quality as a function of the incident laser beam characteristics, the material of the photocathode, and the shape and strength of the accelerating and focusing electric fields in the electron gun.

1.2.1. Objectives

- Develop methods for measuring photocathode performance, particularly the brightness of the emitted electron beam.
- Design, set up, and test a system that emulates the first stage of the DTEM.
- Demonstrate measurements on the DTEM's baseline tantalum cathode.
- Improve the brightness (as defined in Section 2.1.1) of the emitted electron beam by varying the incident laser beam characteristics, the material of the photocathode, and the shape and strength of the accelerating and focusing electric fields in the electron gun.

1.2.2. Constraints

- The design must closely emulate the actual DTEM upper column and utilize the primary components supplied by LLNL. Key components include the vacuum chamber and pump, the cathode laser system, and the electron gun.
- Safety requirements must be met for safe operation. Hazards include high-power lasers, high voltage systems, and x-ray generation.
- Beam alignment must be maintainable in order to produce reliable results.
- Potential photocathode materials must be able to withstand continuous operation for extended periods.

1.3. DELIVERABLES

By the end of the fall semester, the team generated:

- Finalized design plans for both the beam line and the vacuum chamber internals
- Project Documentation and Media, including:
    - Fall Design Reviews
    - Work Plan
    - Midyear Report

By the end of the spring semester, the team delivered the following:

- Primary deliverable
    - A fully functional and automated test setup

- Project Documentation and Media, including:
    - Final Report
    - Spring semester presentation
    - Project day presentation and poster
    - Test Setup Assembly Instructions

2. BACKGROUND

2.1. DTEM

The DTEM is a standard TEM modified with two lasers; these lasers allow the DTEM to examine fast material processes by driving a desired change or transformation in the sample and then imaging the process using a high density pulse of electrons sent shortly thereafter. One laser is responsible for driving the sample ("drive" or "pump" laser), while the other laser ("probe" or "cathode" laser) generates an electron pulse via photoemission from the cathode (a small tantalum disk). The DTEM also has a modified column of electron optics capable of controlling the high intensity electron pulse generated by the cathode laser. After the cathode laser strikes the cathode, the electrons are collimated through the Wehnelt cylinder, accelerated through a series of anodes, and focused onto the sample using magnetic lenses. The electron beam passes through the sample to a CCD below, where the image is recorded. This single shot technique is capable of bringing 10^9 electrons at 200 keV to the sample in a 10-15 ns pulse (Armstrong, et. al.)!

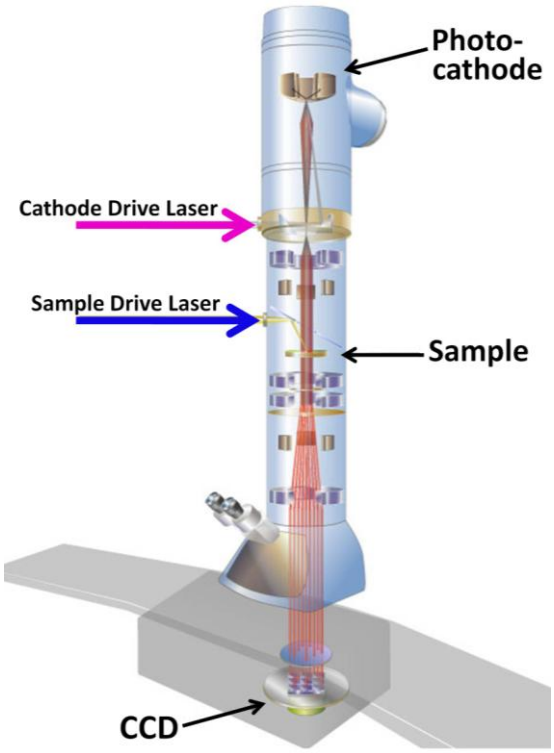

M.R. Armstrong et al. / Ultramicroscopy 107 (2007) 356–367

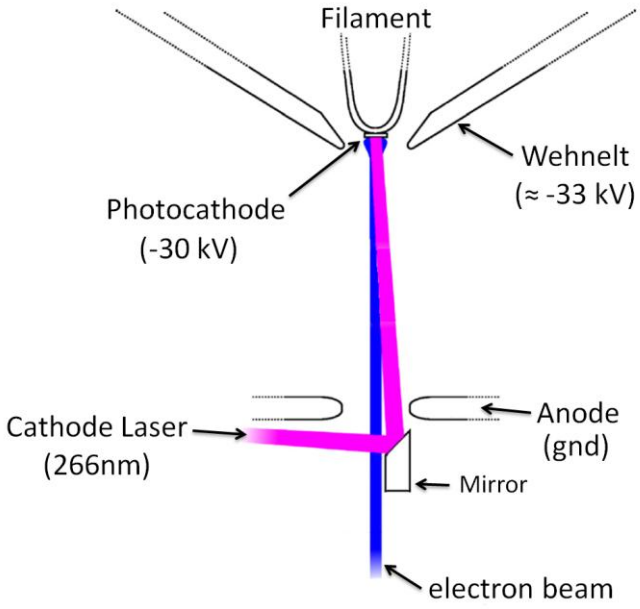

M.R. Armstrong et al. / Ultramicroscopy 107 (2007) 356–367

Figure 1 (Left): Schematic of the DTEM. The hydro-drive laser drives the sample, while the cathode-drive laser generates the electron pulse.

Figure 2 (Right): Electron gun schematic. The cathode laser pulse reflects off a mirror and hits the photocathode to release the electron pulse (not to scale). Note that the photocathode is attached to a tungsten filament which is the standard thermionic electron source for a TEM.

In order to generate 10^9 electrons within a 10 ns window, the cathode laser is a Q-switched Nd:YLF frequency-quintupled to 211 nm. In contrast, the drive laser is a Q-switched Nd:YAG incident upon the sample at either the 1064 nm fundamental frequency or at a frequency-tripled 355 nm. Both lasers have a full-width half-maximum (FWHM) of less than 15 ns for each pulse (Armstrong, et. al.).

The current limiting factor for improving the DTEM is the electron gun system (cathode, Wehnelt cylinder, and first anode). The propagation of the electron beam from the gun to the CCD is already well understood. Likewise, there are no significant improvements that can be made to the current laser system. A new laser system is in development; however, the full potential of this new system cannot be realized without improvements to the electron gun system paired with a better understanding of the system itself. The performance of the electron gun system will primarily be measured in terms of the brightness of the emitted electron beam. As mentioned in the problem statement, brightness is affected by the beam profile of the laser used to eject electrons from the cathode, the material properties of the photocathode, and the voltage and spacing of the initial beam accelerating components. A detailed explanation of brightness follows.

2.2. TERMINOLOGY

2.2.1. Brightness

The electron gun system is important because it is responsible for determining the upper limit on the number of electrons in the beam as well as the upper limit on the beam quality. These two factors are combined into a quantity called brightness. For our purposes, brightness is the charge per unit area per unit solid angle per unit time and is given by the formula,

$$B = \frac{Ne}{(\pi r^2)(\pi \alpha^2)\Delta t},$$

where N is equal to the number of electrons per pulse, e is the charge of an electron, r is the beam radius, α is the angle of convergence, and Δt is the pulse duration (Reed, et. al., "The Evolution of.."). For an image, N determines the number of possible distinct pixels in an image and r specifies the region of interest on which those pixels are focused (the amount of magnification). For example, a 1000 by 1000 pixel image at 8 bits per pixel will require $1000*1000*2^8 = 2.56e8$ electrons at minimum. If the electron beam for this 1000 by 1000 pixel image were focused so that each pixel was equivalent to a square nanometer on the sample, then r would be approximately 500 nm. Intuitively, α determines how many of the 2.56e8 electrons will pass from the 1 nm square on the sample to the corresponding pixel on the CCD (ignoring the additional scattering that would result from impact with a sample). A low α means electrons have low transverse velocities and tend to impact the correct location on the CCD. A high α reduces the sharpness of the image.

Brightness is extremely important because it is semi-conserved in a passive system like the DTEM; that is, the brightness of the beam as it is emitted at the cathode must be greater than or equal to the brightness of the beam when it encounters the sample (Reed, et. al., "The Evolution of…"). For imaging purposes, a larger brightness means more electrons and/or a better beam profile (smaller solid angle)—both result in an improvement in the resolution and contrast of the final image. Note that it is possible to degrade the beam brightness through space-charge effects and scattering, but there is no way to improve brightness in a passive system.

2.2.2. Coherent Fluence

An alternate way to examine the electron beam is to use the quantity coherent fluence. Coherent fluence is a dimensionless quantity that removes the time dependence of brightness by multiplying by the factor Δt, and accounts for the variation of brightness through an accelerating voltage by including the term λ^2. The expression is,

$$N_c = \frac{N\lambda^2}{r^2\alpha^2} = \frac{\pi\lambda^2 B\Delta t}{e},$$

where N is the number of electrons in the pulse, λ is the electron wavelength, r is the beam radius, α is the local convergence angle, B is brightness, Δt is pulse duration, and e is the charge of an electron (Reed, et. al., "The Evolution of.."). The end result is that N_C is proportional to the number of electrons per spatial coherence area per pulse. As a measure of electrons per coherence area, N_C reveals the capability of an electron beam to be used for coherent imaging. A value of N_C less than 10 implies that the beam cannot be used for coherent diffraction imaging (an imaging technique in which the diffraction pattern of the incident beam is used to reconstruct a high resolution image of the sample) (Reed, et. al., "The Evolution of.."). Like brightness, no passive system can improve the beams coherent fluence as it propagates to the sample. The current system produces a beam with an N_C value of 1, which is only suitable for incoherent imaging.

Since brightness and N_C are conserved, they determine the upper limit on the quality of the beam used to produce an image. Improving and understanding the electron gun system is the next step to improving the DTEM.

3. IMPACT

The purpose of the team's test setup is to make advancements in microscopic fast-exposure imaging. The DTEM is the only TEM that can take nanosecond-scale exposures and still get meaningful resolution (Reed, et. al). The current microscope at LLNL will soon be updated with a more powerful laser and a better focusing system. Once these improvements to the current setup have been made, the weak point of the revised DTEM will be the electron source. Thus, to further improve the upcoming setup, the photocathode must be optimized. The team's test setup hopes to achieve this by providing a means for finding the best photocathode setup to produce a high brightness electron beam for the DTEM. This project involves technologies and applications from many different sides of both engineering and physics, challenging the team to combine various fields of study into this one application.

The DTEM currently uses a tantalum photocathode. The tantalum photocathode has proven to be very durable, but a material which can produce a higher intensity and higher brightness electron beam is desirable. Many other variables such as cathode laser spot size and Wehnelt voltage are also of interest. An improved electron microscope will allow for higher resolution and higher contrast images of the materials and processes captured by the microscope. Improvements in image quality will allow for a better understanding of many phenomena ranging from martensitic phase transformations to radiation damage in organic molecules. The DTEM allows for the examination and analysis of phase transformations and dislocation dynamics in structural

materials, as well as solid state reactions such as diffusion in thin films. It also enables the examination of catalytic reactions, such as nanowire and nanoparticle growth, and biological processes such as pathogen identification. The ability to catch these rapid processes in action with the DTEM has enormous potential for future applications in physics, materials science, chemistry, and biology (Reed, et. al., "Nanosecond Dynamic…").

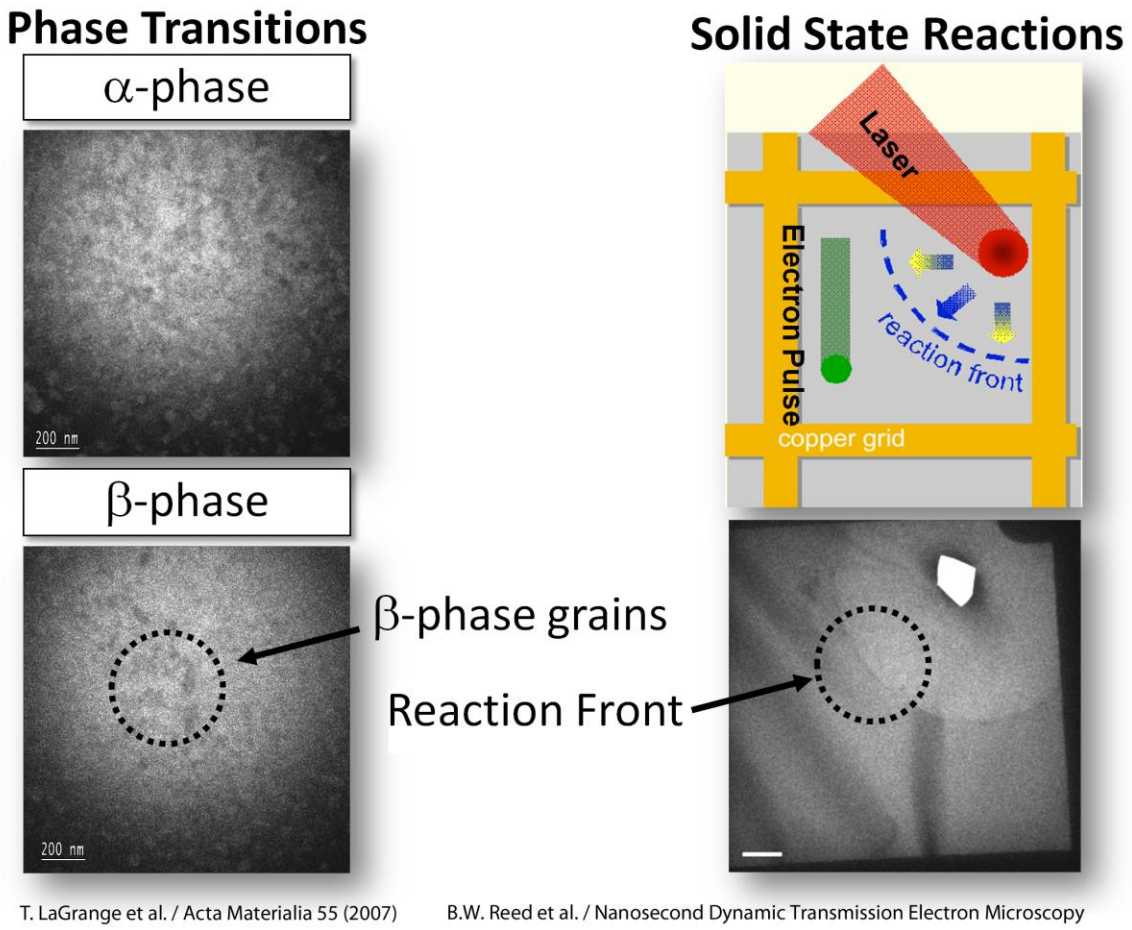

Figure 3: Examples of DTEM applications. At left, β-phase grains appear during a martensitic reaction. At right, a multilayer foil reaction propagates outwards after initiation from the sample drive laser which appears as a white void in the image.

4. DETAILED DESIGN

4.1. LASER

The laser is a Spectra-Physics GCR-190 Nd:YAG. It is Q-Switched with a maximum power per pulse at 10 Hz. It outputs approximately 500 mJ per each 10 ns pulse in a 9 mm diameter beam. The laser head has a built in frequency doubling crystal housing. After phase matching the crystal and tuning the polarization into the crystal, the laser outputs slightly less than 100 mJ per 7 ns pulse at 532 nm. These statistics are below the OEM specifications, but they are still a great improvement over the state of the laser at the beginning of the year. When we received the laser, the beam profile was a half moon, and the power was approximately 100 mJ per pulse at 1064 nm at 10 Hz. To improve the power, the elliptical reflectors for both the oscillator and the single-pass amplifier were removed and cleaned. After cleaning, the beam profile was slightly improved and the power was about 400 mJ per pulse at 1064 nm at 10 Hz. To fully fix the beam profile, we carefully adjusted the alignment of the oscillator. After re-aligning the oscillator, we achieved the current radially symmetric cut-off Gaussian beam profile and 500mJ pulse power. These modifications were suggested and overseen (by phone) by Javier Soto at Spectra-Physics. The uncovered laser head can be seen in Figure 4.

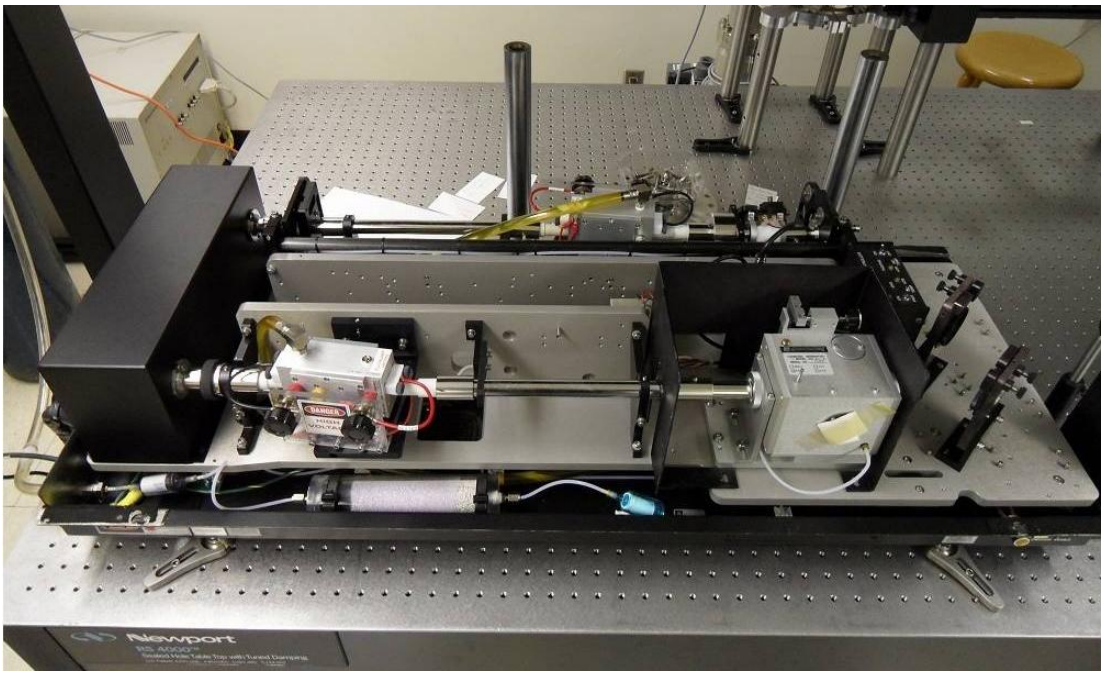

Figure 4: A photo of the uncovered laser head. The single pass amplifier (left) and internal frequency doubling module (right) can be seen in the foreground. On the other side (background) of the laser head is the oscillator and Q-switch. Note the temperature controller for the frequency doubling module, seen at the right of the module. In the background (left), the laser power supply is visible.

4.2. OPTICS

The 1064 nm output of the Nd:YAG laser is frequency doubled to 532 nm using an internal module inside the laser head. The image of the beam on the face of the internal second harmonic crystal is then relay-imaged onto the face of the external second harmonic crystal using a 50 cm focal length lens and a 35 cm focal length lens placed confocally. This serves the dual purpose of reducing the beam diameter to approximately 6.5 mm (so that the entire beam fits within the external doubling crystal) and ensuring that the beam incident upon the external doubling crystal is collimated (improving the frequency conversion efficiency). Using a pair of turning mirrors, the beam is raised to the level of the vacuum chamber and passed on to the focusing system. The

focusing system consists of a diverging lens with a focal length of -10 cm, a converging lens with a focal length of 50 cm, and a converging lens with a focal length of 35 cm. The f = -10 cm and f = 50 cm lens form a Galilean beam expander that increases the beam diameter to 3.5 cm. The f = 35 cm lens is used to focus the expanded beam down to a spot on the photocathode. Expanding the beam before focusing down is necessary to reduce the diffraction limit below our goal of a 10 micron diameter spot on the photocathode. See Figure 6 for a schematic of the beam line.

To ensure that the laser is outputting the expected power and that the beam is properly aligned on its path to the cathode, various controls and checks are placed along the beam line. The control elements allow safe manipulation of the beam. A Uniblitz shutter controls when the laser beam is allowed to pass into the vacuum chamber, and a 266 nm half-wave plate paired with a thin film polarizer allows for adjustment of the beam power. These three elements are placed after the external 266 nm producing second harmonic generator (SHG) in the beam line so that the laser can continue to rep into the crystal at full power even if the beam is attenuated or stopped before entering the vacuum chamber. This keeps both the laser and crystal at a steady state temperature. When the laser is not in use, the external SHG is kept in a desiccant enclosure. See Figure 5. When the laser is in use, dry nitrogen is blown on the crystal at all times. A 532 nm half-wave plate placed before the SHG allows adjustment of the polarization of the 532 nm light incident on the SHG so that conversion efficiency can be maximized. Beam stops have been placed behind mirrors to block stray light.

Figure 5: A photo of the second harmonic crystal used to double 532 nm light to 266 nm light. In the photo, the crystal is not in use and therefore it is in its desiccant jar. While in operation, the jar is removed and dry nitrogen is blown across the crystal.

The diagnostic elements ensure that the beam has the expected power and alignment. A power meter provides power readings just after the last turn, a centering camera ensures that the beam is centered as it enters the final stretch of focusing optics, and a pointing camera allows monitoring of the laser spot size and position as it strikes the cathode. A photodiode is used to capture temporal measurements of the beam pulses. Light for the power meter and photodiode is provided by a 3 degree wedge sampler. Measurements taken from the wedge sampler will need to be calibrated against in-line readings taken from the full beam. In-line measurements will need to be repeated routinely in order to accurately characterize the beam since the power meter

and photodiode have reduced accuracy when measuring the sampled beam which contains less than 1% of the total beam power.

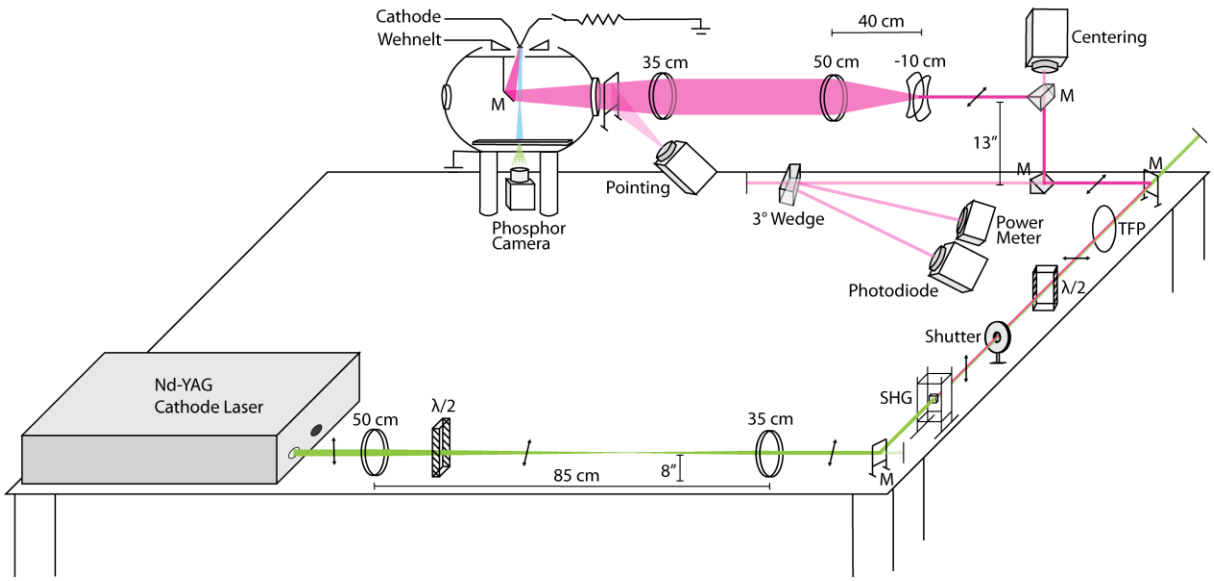

Figure 6: The laser (Spectra-Physics GCR-190) contains an internal harmonic generator that doubles its 1064 nm fundamental output to 532 nm. The transverse beam profile from the laser's internal crystal is then reduced by a factor of 1.4 and imaged onto the external second harmonic generator using a 1.4:1 relay consisting of a 50 cm and 35 cm lens. The second nonlinear crystal outputs fourth harmonic light at 266 nm. The 512 nm light is dumped and the 266 nm light is expanded and then focused down, passing into the vacuum chamber where it is reflected by the cathode mirror onto the cathode where it forms a focused spot (less than 20 microns in diameter). The beam is expanded using a diverging lens with focal length f = -10 cm and a collimating lens with f = 50 cm. An f = 35 cm objective lens focuses the expanded beam onto the cathode. It is necessary to expand the beam in order to get the solid angle required to achieve a 20 micron or better beam spot on the cathode. The components needed for the beam line are detailed in Table 1. Note that the beam spot size on the cathode will be varied by translating the diverging lens in the focusing system. Also note that the vertically polarized 532 nm light from the laser is turned 45° as it is relayed onto the external SHG. This rotation is necessary so that the type II external SHG can combine pairs of photons with orthogonal polarizations into single photons with extraordinary polarization (vertical).

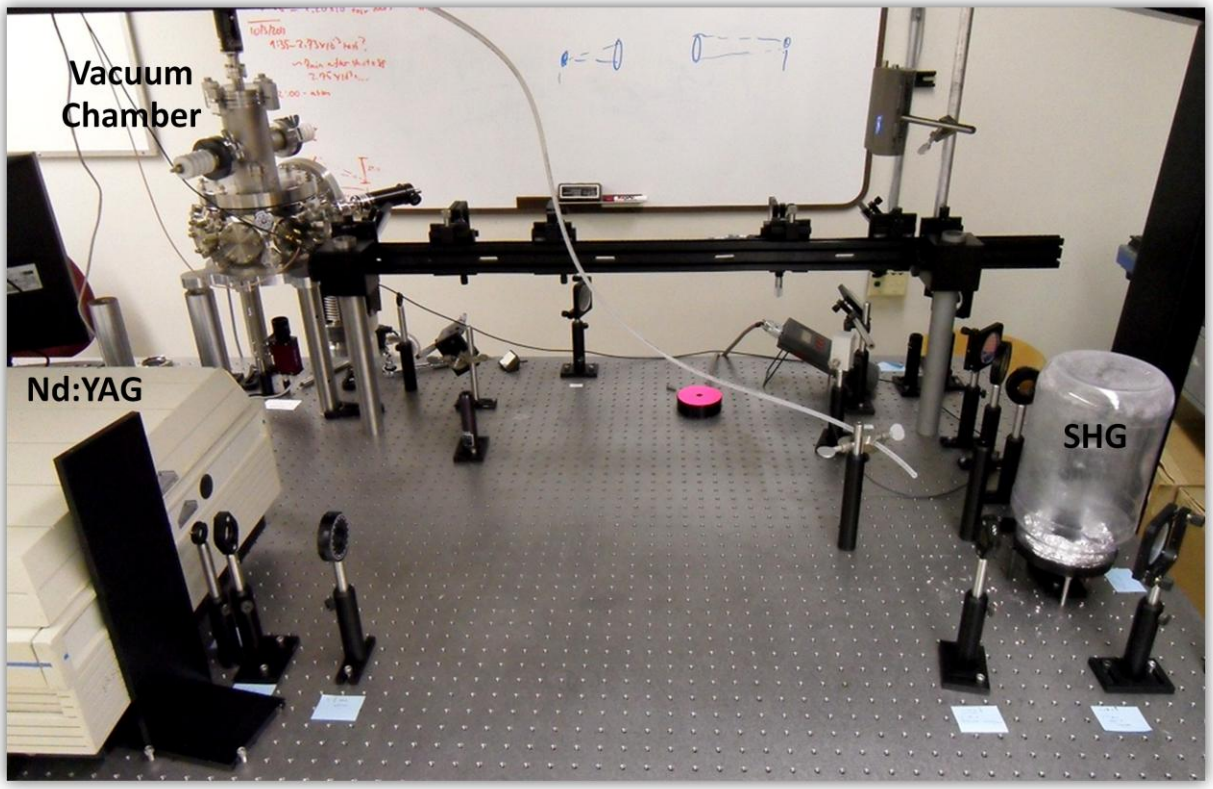

Figure 7: Image of the nearly completed optics path. This image corresponds to the schematic in Figure 6.

Table 1 – Components used in the beam line.

Component	**Description**
Spectra-Physics GCR 190 Nd:YAG Laser	Focused onto the cathode to generate an electron beam
Fourth Harmonic Crystal	Takes the 532 nm output of the laser and doubles it to 266 nm
Uniblitz Shutter	Controls when the laser is let into the beam line
Half-Wave Plate (266 nm)	Modulates beam power in conjunction with the thin film polarizer
Half-Wave Plate (532 nm)	Maximizes conversion efficiency through the fourth harmonic crystal
Thin Film Polarizer (266 nm)	Modulates beam power in conjunction with the half-wave plate
(2) x Dielectric Mirrors, p-Polarized (532 and 266 nm)	Used to bend the beam path so it fits on the 8’ x 4’ optics table
50 cm Converging Lens (532 nm)	Along with the 35 cm converging lens, this lens forms the relay that

	takes the beam profile from the second harmonic crystal and images it at 3/5 size onto the fourth harmonic crystal
35 cm Converging Lens (532 nm)	Along with the 50 cm converging lens, this lens forms the relay that takes the beam profile from the second harmonic crystal and images it at 3/5 size onto the fourth harmonic crystal
(2) x Dielectric Mirrors, s-Polarized (266 nm)	Used to raise the beam path height so it can pass into the vacuum chamber
Power Meter	Used to determine power in the beam
Photodiode	Used to determine temporal profile of the beam
Centering Camera	Used to align the beam through the optics in the beam path
Pointing Camera	Used to center the beam on the cathode as well as determine beam size on the cathode
-10 cm Diverging Lens (266 nm)	First lens in the focusing system, used to expand the beam
50 cm Converging Lens (266 nm)	Second lens in the focusing system, used to collimate the beam
35 cm Converging Lens (266 nm)	Final lens in the focusing system, used to focus the beam

4.3. POWER SUPPLY

To function properly, the electron gun requires a voltage of -30 kV to be maintained at the filament (cathode) while a voltage of 0 to -3.3 kV relative to the cathode is maintained at the Wehnelt. The 30 kV difference between the -30 kV cathode and the anode at ground (0 V) provides the accelerating force for the electron beam. The adjustable voltage difference between the Wehnelt and the cathode provides preliminary focusing for the electron beam just as it is emitted from the filament.

The power supply which the team received uses a 0 to -35 kV power module for the cathode, and a floating ± 3.5 kV module for the Wehnelt. The floating module was configured to take the cathode voltage as input and provide ± 3.5 kV relative to that voltage. Unfortunately, the floating module was unable to provide the stated output voltage range so the team worked out a plan with

resident electronics expert Walter Cook to run both the cathode and Wehnelt voltage outputs off of the fully functional cathode power module. Walter Cook has implemented the new setup and confirmed its functionality. As before, the cathode output on the new setup simply delivers the voltage to which the 0 to -35 kV cathode power module is set. The Wehnelt output, however, is now tied to the resistor step down ladder for the same power module. A switch allows the user to change the location on the voltage divider of the Wehnelt output – it functions just like a potentiometer except it provides incremental outputs. By adjusting this dial, the Wehnelt output can be swung from the top of the ladder, where it delivers the same voltage as the Cathode, to the bottom of the ladder, where it delivers a voltage which is 10% lower. The ladder is composed of ten resistors in series such that the Wehnelt voltage can be adjusted from 90-100% of the cathode voltage in 1% increments. For example, if the cathode power module is set to -30 kV, the ladder allows the Wehnelt to be set to -29.7, -29.4, -29.1, -28.8, -28.5, -28.2, -27.9, -27.6, -27.3 or -27 kV. See Figure 8. Since the electron gun functions with the Wehnelt set to a more negative voltage than the cathode, the cathode and Wehnelt leads have been switch. Thus, the Wehnelt output is sourced directly from the cathode power supply, and the cathode output is the stepped down voltage. The only drawback to the new setup is that the adjustment dial is now internal and the power supply must be powered down before the setting can be changed. Since typical test setup operation does not require frequent adjustment of the cathode or Wehnelt voltage, this is only a minor inconvenience however.

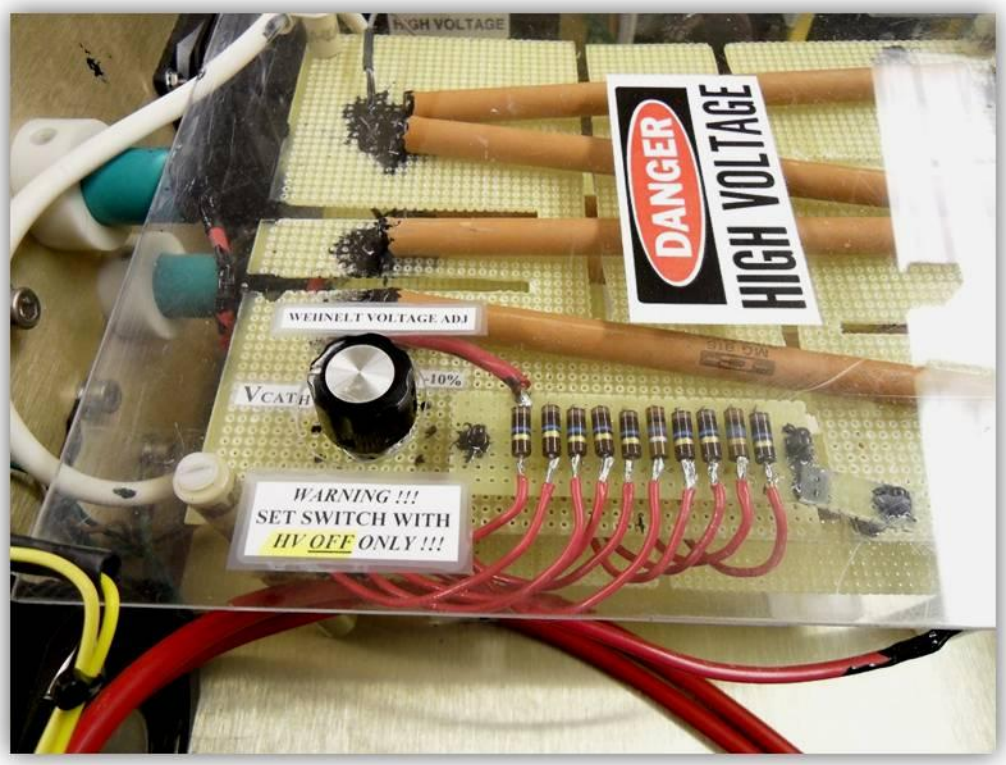

Figure 8: This is a photo of the variable step down circuit used to vary the voltage between the Wehnelt and the cathode. The knob determines the overall voltage difference by changing the number of resistors the current passes through.

4.4. VACUUM CHAMBER

Figure 9 shows an external view of the vacuum chamber and electron gun and Figure 10 shows a simplified cross section of the vacuum chamber internal layout. The chamber is a Kimball Physics 8.0” Extended Spherical Octagon. The electron gun rests on top of the chamber and the camera images the electron beam from below the chamber as the beam strikes the phosphor screen lying on the chamber floor. Seven of the available eight 2.75” diameter conflat ports are used for this setup. One is fitted with a window through which the cathode laser enters the chamber. Another is fitted with a linear actuator which allows a Faraday cup to be moved into

the electron beam path. See Figure 12. The third is fitted with a motor-actuated linear translator for moving an aperture to sample across the electron beam and the fourth conflat port is used for the vacuum pump pressure sensor. A fifth 2.75" conflat port is used for a feed-through so that charge readings from the Faraday cup and the beam sampler can be passed to the computer. The sixth port is used to mount the turning mirror in the vacuum chamber (Figure 11). The chamber is evacuated through the seventh 2.75" conflat port. Additionally, a vacuum interlock is installed on a conflat mini port. The vacuum interlock will trip if there is a loss of vacuum, cutting power to the high voltage power supply so that prolonged arcing does not occur between the Wehnelt and anode inside the chamber.

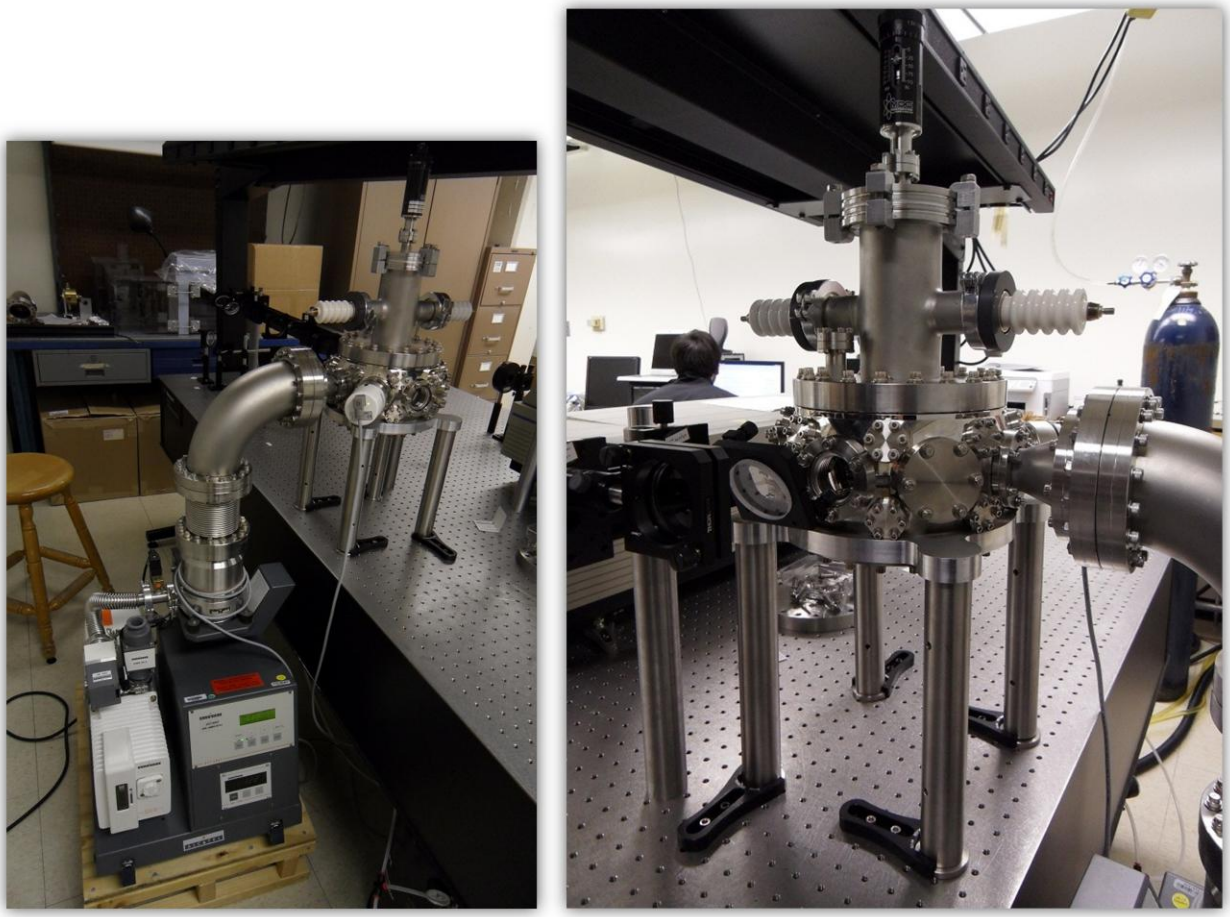

Figure 9: External view of vacuum chamber and vacuum pump (left). Close-up view of chamber (right). Note the electron gun mounted on top of the chamber with high voltage leads on left and right and a linear translator at the top for adjusting the distance between the anode and the wehnelt/cathode assembly. The optics components (visible on the left of the close-up picture) are the final objective lens and beam sampler. The cathode laser beam passes into the vacuum chamber through the window just beyond the beam sampler.

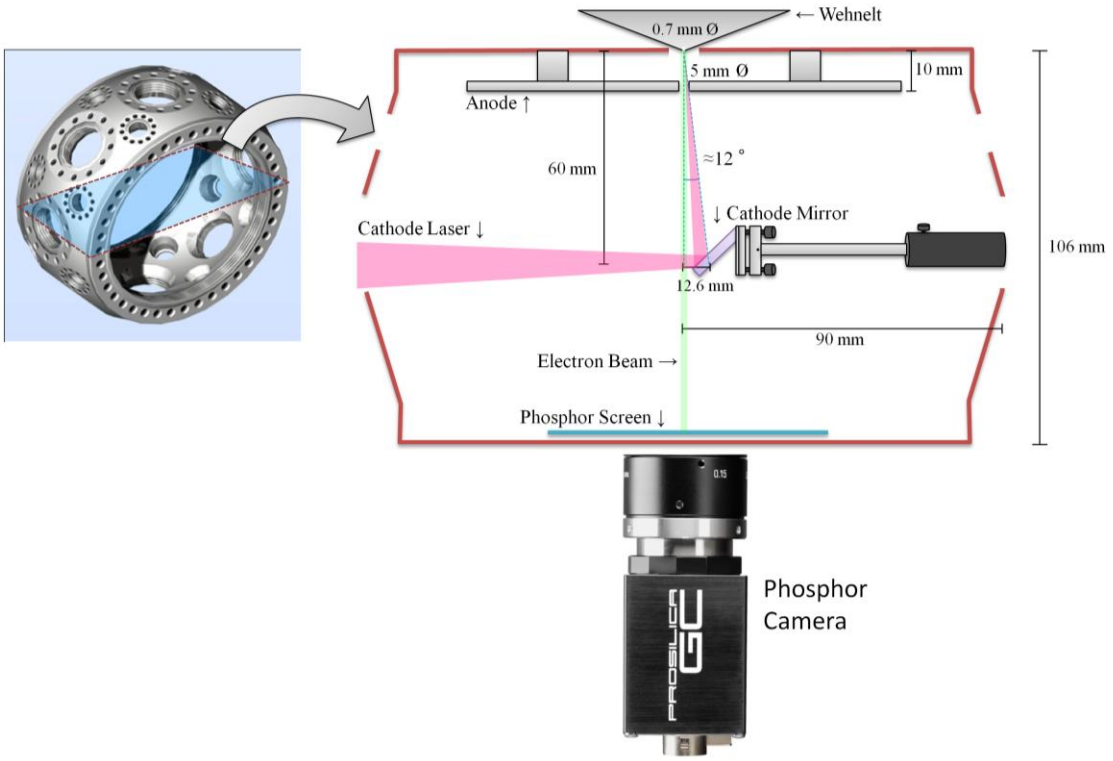

Figure 10: Schematic of vacuum chamber internals. Note the tight clearance for the laser as it passes through the anode into the Wehnelt.

As shown in Figure 10, the narrow margin for the cathode laser as it passes from the cathode mirror through the anode and into the Wehnelt posed a significant challenge with the vacuum chamber setup. A photo of the inside of the chamber can be found in Figure 11.

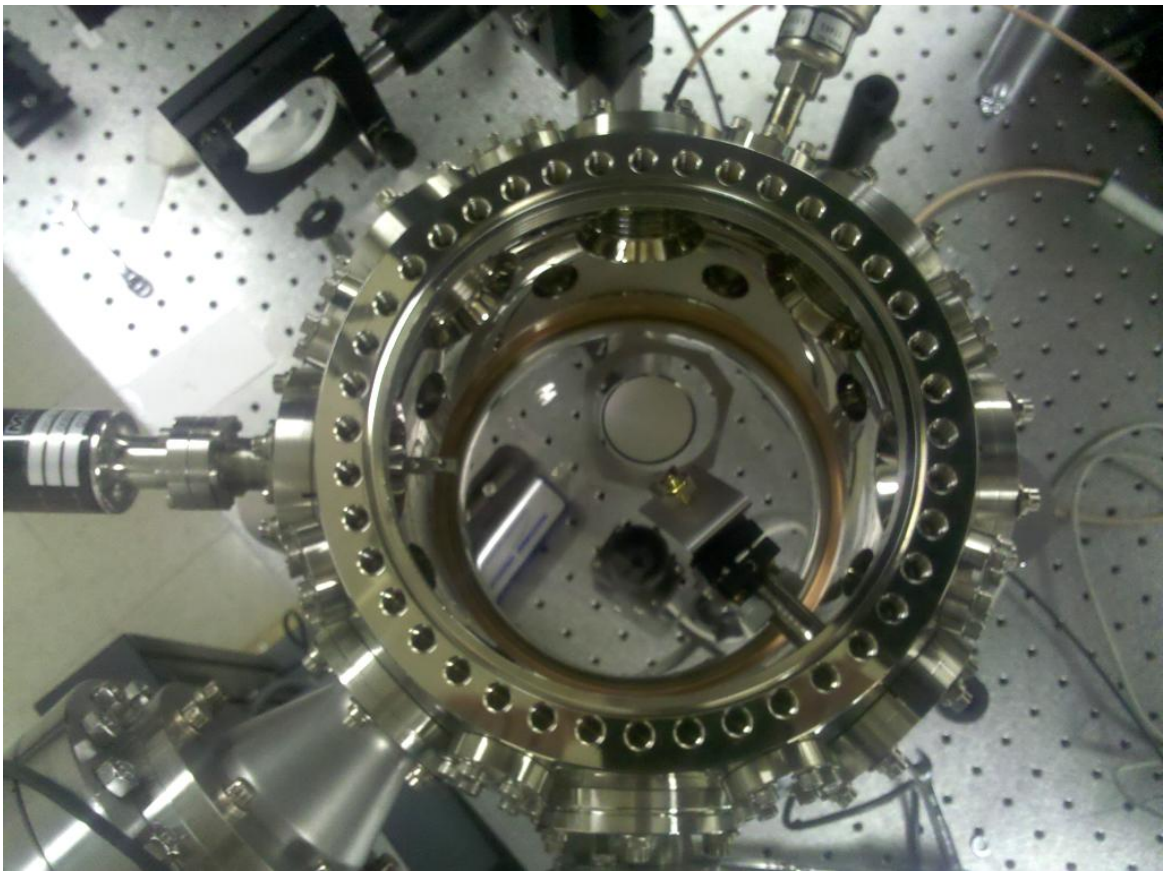

Figure 11: A photo from the top of the uncovered vacuum chamber. The mirror mount and mirror can be seen in the lower right-hand corner of the chamber. The phosphor screen is at the top of the chamber floor. The sheet metal ring around the phosphor screen allows a magnet to be used to move the phosphor screen around the chamber when the chamber is closed. The linear feedthrough for the Faraday cup is at the left of the chamber. The phosphor camera can be seen through the window on the bottom of the chamber. Not pictured here are the Faraday cup, the motor controlled linear feedthrough, and the beam sampler.

Figure 12: A picture of the Faraday cup. Note how it is mounted on non-conducting material. This is to ensure that the charge readings taken from the cup are correct.

4.4.1. Vacuum Interlock Circuit

The vacuum chamber must be equipped with a vacuum interlock circuit to prevent arcing from occurring between the anode and wehnelt when there is a loss of vacuum. In order to cut power to the high voltage power supply when there is a rise in vacuum chamber pressure, the team purchased a thermocouple pressure gauge (model TGT-1518M) and devised a circuit that would be able to detect a change across a threshold voltage, as shown in Figure 13. The thermocouple draws a heater current of 15 mA, measures pressures down to 1e-4 torr, and has a response time of .1 seconds. The response time of the thermocouple may not be fast enough to prevent arcing in the event of an extremely rapid loss of vacuum, but it will prevent prolonged arcing and x-ray

generation. The power supply is also current limited by design in order to prevent excessive discharge in the event of breakdown.

The interlock circuit is comprised of four sections. The first section supplies a heater current to the thermocouple and reads the voltage from the output pins on the thermocouple gauge tube which represents the pressure inside the chamber. This voltage is then passed through an adjustable gain op-amp circuit. The modified voltage is then compared to a known reference voltage, which is stabilized using the voltage follower circuit. These are compared using a voltage comparator. The output of the circuit will either be positive or negative depending on which input port of the op-amp is higher. If the output voltage's sign suddenly changes, the relay supplying 24 V power to the high voltage supply would then be tripped by the system, disconnecting power.

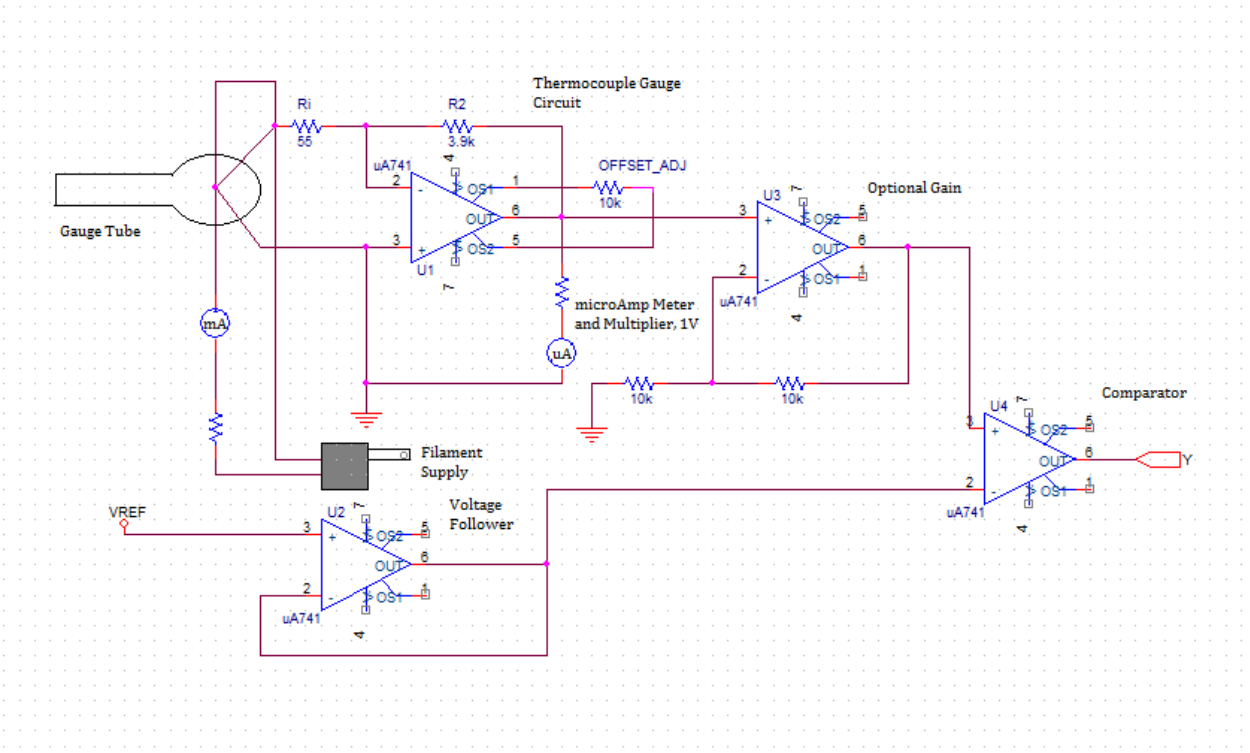

Figure 13: A proposed schematic for the thermocouple comparator circuit. The circuit is composed of four sections – a gauge circuit used to measure pressure, a voltage follower for the reference voltage, an optional gain circuit, and a voltage comparator circuit.

4.4.2. Mirror Mount and Mirror

A half inch post holder, half inch post, compact kinematic mount, and a metal bracket are used to mount the mirror in the vacuum chamber. One side of the post holder was milled down and a modified thumb screw was machined so that the post holder would fit within the chamber. A graduated 1.5" post attached to a compact kinematic mount is used to hold the mirror bracket. A 39^{o} sheet metal bracket is used to attach the mirror to the mount. The mirror is clamped to the bracket using a nut and bolt. Since the cathode laser is constrained to an angle of 12 degrees from vertical, the mirror edge is very close to clipping the electron beam. Thus, an aluminum coated mirror is used so that stray charge does not accumulate on the mirror and introduce

irregularities into the electron beam. The mirror is grounded through its attachment to the mirror mount. The resistance to ground was measured at 2.5 ohms between the mirror face and the base of the post.

4.4.3 Beam Sampler

To determine brightness, an accurate profile for the electron beam intensity as well as angle of convergence needs to be acquired. The team plans to achieve this by sweeping an aperture across the electron beam. The current configuration consists of a 50 micron aperture attached to a servo controlled linear translator which sweeps the aperture through the beam while frames are acquired from the phosphor camera. The ~50 micron apertures allow only small sections of the beam to pass through to the phosphor screen below. Upon impact by the emitted and passed electrons, the phosphor screen phosphoresces, providing a measurement of the local divergence of the beam (see Figure 14). Additionally, once the fluorescence of the phosphor screen is calibrated against the Faraday Cup, the total current contained at the sampled beam location (as well as the local distribution of current as a function of divergence) can be calculated using the brightness of the acquired pixel values. Lastly, the electron charge accumulated on the aperture setup can then be taken out of the vacuum chamber via a feedthrough. The team can form an intensity profile for the electron beam by calculating the charge carried within each sliver of the beam intersected by the beam sampler as it is moved across the beam face. This will be useful for cross-checking results from the phosphor screen and verifying the symmetry of the beam.

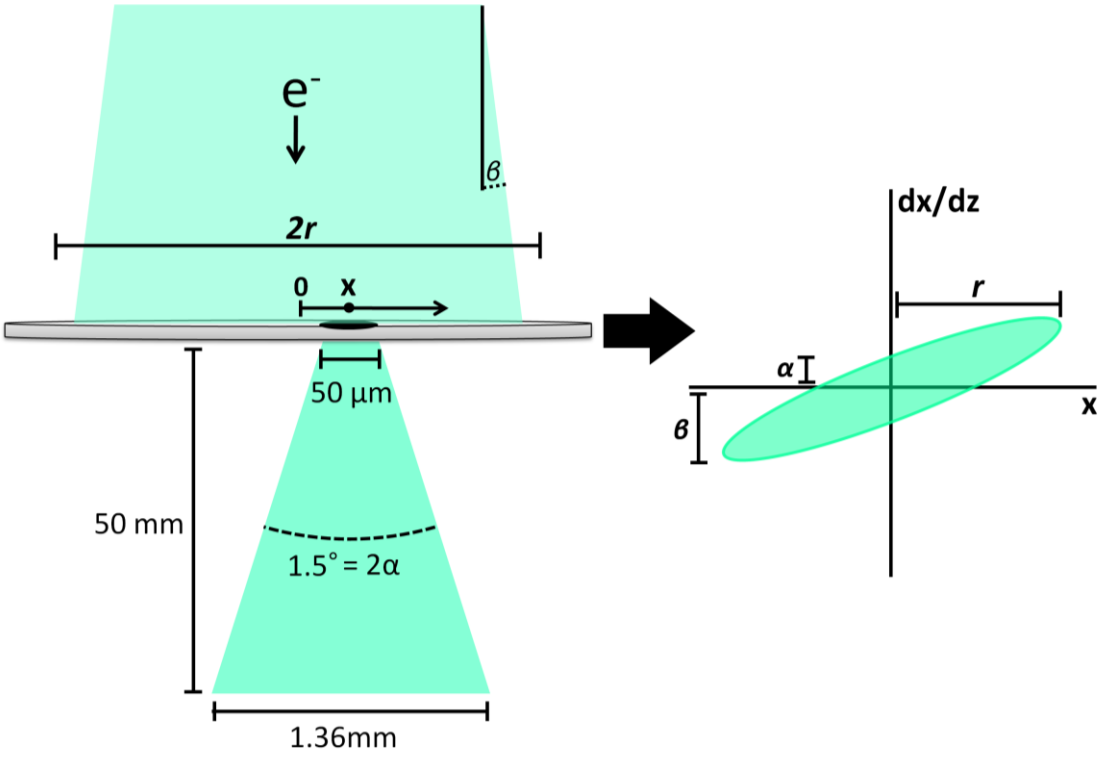

Figure 14: A small aperture samples the electron beam. The local angle of convergence/divergence can be calculated from the profile of the sampled beam on the phosphor screen. Also, the charge distribution of the beam can be computed by measuring the charge accumulated on the beam sampler as a function of the sampler's position within the beam.

4.4.4 Phosphor Screen

The team has purchased a custom phosphor screen for acquiring images of the electron beam profile. The screen is 4 cm diameter plate of glass coated with 1.4 mg/cm^2 of P43 phosphor. The phosphor is vacuum compatible and aluminized so that the screen can be grounded to prevent charge buildup from the incident electron beam. The phosphor particle size is 2-3 microns and provides 20 micron resolution. The pairing of a glass substrate with a thin phosphor layer allows the phosphor camera to capture the screen's fluorescence from the screen's

backside. This capability allows the team to place the phosphor camera directly below the vacuum chamber where it can acquire on axis images of the screen without the use of angled objectives or a complex mirror system.

4.4.5 SMA Feedthrough

In order to acquire data from the Faraday cup and beam sampler, the team installed an SMA feed through in the vacuum chamber. To cut costs, the team purchased three surplus SMA bulkhead female to female connectors and fitted them to a blank conflate 2.75" flange. The 50 ohm connectors are hermetically sealed and have 18 GHz bandwidth. The flange was machined to accept the connecters which form a seal with Viton O-rings. The chamber was pumped down to 10^{-6} torr with the feedthroughs installed to verify that they are suitable for the vacuum requirements of brightness testing.

4.5. ELECTRON GUN

The electron gun provided for the team by LLNL is a duplicate of the electron gun currently operating in the DTEM. This ensures that brightness measurements acquired with this hardware will be relevant to the DTEM group. The gun has high voltage leads for the Wehnelt and cathode as well as a linear translator which moves the Wehnelt and cathode up and down along the emitted beam axis relative to the anode. This changes the density of the accelerating field. Figure 15 shows the Wehnelt and original anode.

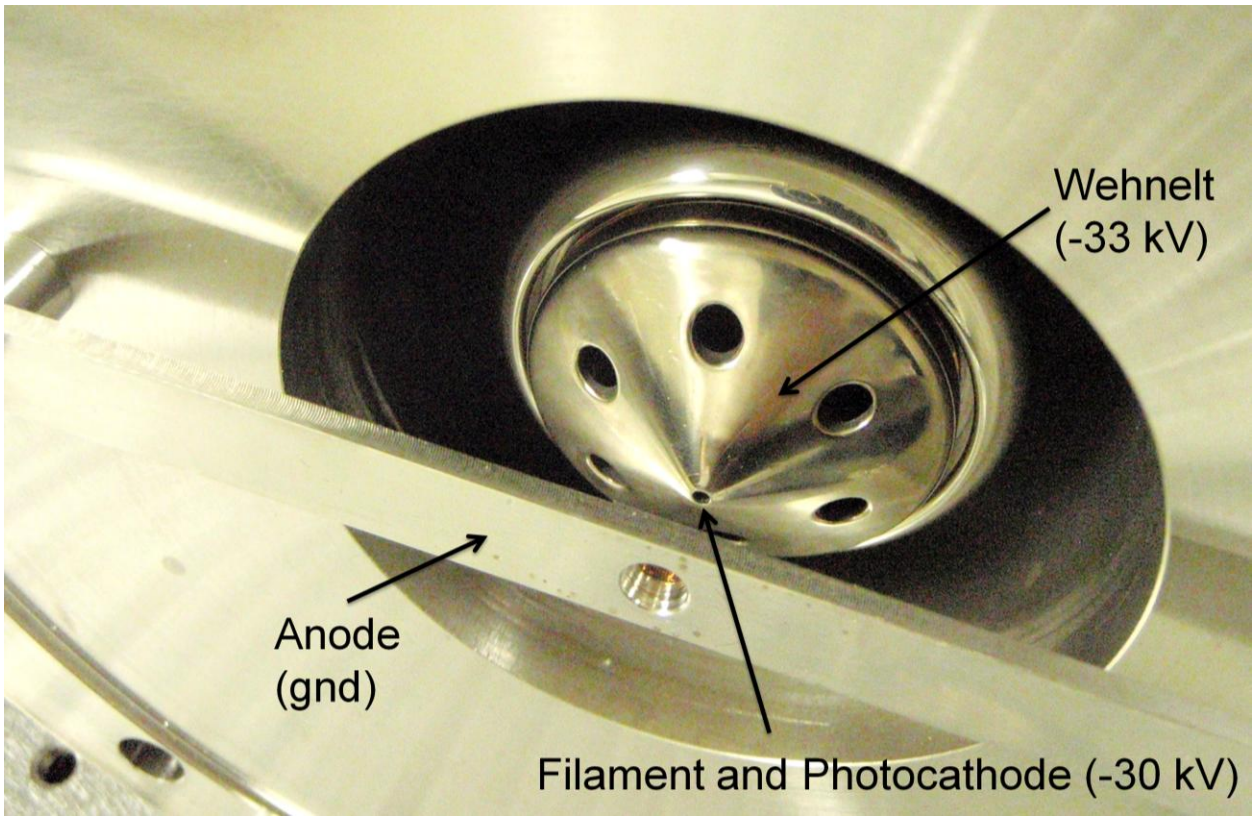

Figure 15: Image of the key components of the electron gun. The photocathode (not visible) sits just behind the opening in the tip of the Wehnelt.

Two modifications were added to the electron gun to improve electron beam quality. First, the rectangular anode shown above was replaced by a custom machined disk-shaped anode shown in Figure 16. This new anode ensures that the accelerating field produced by the anode is radially symmetric. The second modification was to insert a high voltage diode between the cathode filament and the wehnelt. When the Wehnelt voltage is lower (more negative) than the cathode, the components remain isolated across the diode, however, if the Wehnelt voltage is set higher than the cathode voltage, the diode allows current to flow through the filament. This allows the team to produce thermionic electron emission while heating up the filament so that it burns the oxide layer off of the cathode. This increases the photoemission efficiency of the cathode. Most

importantly, with the diode installed the oxide layer can be burned off while the system remains under vacuum. The diode isolates up to 5 kV between the Wehnelt and cathode in its reverse direction with less than a microamp of leakage, but passes an amp through the filament with the application of 6 volts in the forward direction.

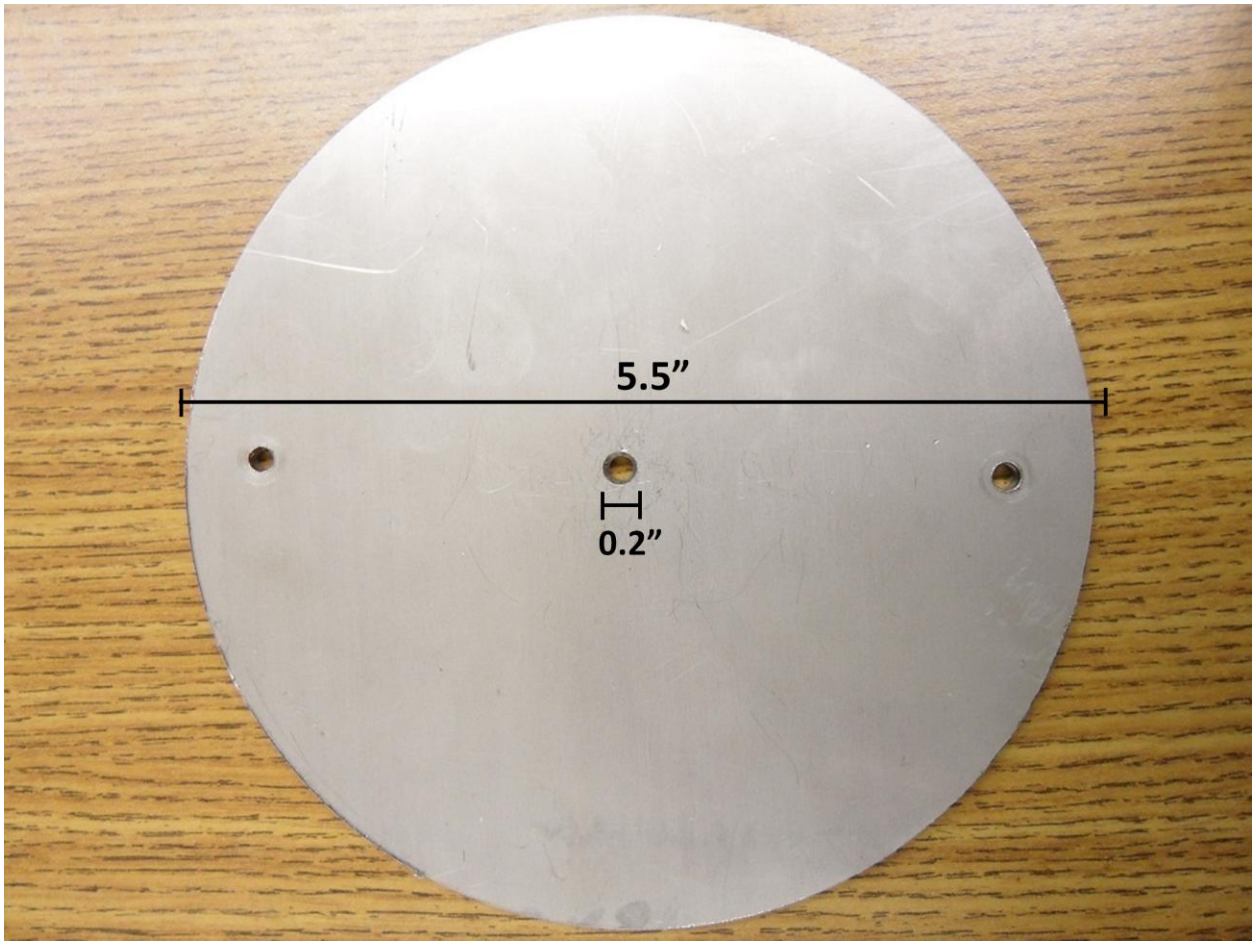

Figure 16: Image of new anode before sanding and polishing. Note that the center hole is tapered to provide clearance for the cathode laser which must pass through the hole in order to reach the photocathode. The accelerating field is produced between the backside of the anode and the cathode, and thus is unaffected by the tapering.

4.6. LabVIEW FRONT PANEL

In order to allow for efficient data collection and organization, a computer workstation was assembled. The workstation manages system operation, device triggering, and data acquisition through a single LabVIEW front panel. Additionally, this VI is responsible for saving well organized test data with headers denoting the test conditions at time of capture. Data processing will be done separately using a series of MATLAB scripts.

4.6.1 Control and Triggering

The LabVIEW front panel generates trigger signals for the cathode laser and Uniblitz shutter. The user inputs a frequency and Q-switch delay and the VI automatically generates the flash lamp and Q-switch pulses needed to fire the laser at the given setting. The pulses are generated with sub-microsecond width and inter-pulse delay using onboard counters on the installed National Instruments DAQ. A few milliseconds before each laser pulse, the VI sends a trigger to open the Uniblitz shutter, in order to allow the laser pulse to pass through. Laser trigger signals are activated by pressing the "Fire!" button, and the "Pass Beam" button activates the shutter trigger, allowing the beam to pass into the vacuum chamber (see Figure 18). The "Grab Data" button initiates data acquisition (described below).

4.6.2 Oscilloscope and Camera Integration

The workstation acquires data from the phosphor camera and its internal 1Gs/s oscilloscope. The scope has two channels, allowing the workstation to capture data from the photodiode as

well as from the Faraday cup or beam sampler. Additionally, the station displays the streams from the centering and pointing camera for monitoring the alignment of the cathode laser.

The pointing and centering camera streams are captured by an Adlink capture card. This capture card decodes the analog video signals from these cameras which have an effective resolution of approximately 640 by 480 pixels. The streams from these cameras can only be accessed via Adlink's proprietary camera preview software since the LabVIEW compatible drivers do not support the workstation's 64-bit Windows 7 installation. Since these cameras are primarily used to check beam alignment, this is an acceptable inconvenience.

The higher resolution phosphor screen camera (an AVT Manta G-201 Monochrome CCD Camera) uses 1000 Mb/s Ethernet to stream data to the computer. The phosphor camera provides 1620 by 1220 pixel images in 12 bit monochrome at 14 frames per second. The camera's 0.55 inch diagonal CCD is positioned approximately 110 mm from the phosphor screen. Using a 25 mm focal length imaging lens at this distance, the camera captures a 1 cm^2 field of view from the phosphor screen. The resulting images have a spatial resolution of 14 microns per pixel. The CCD has excellent light sensitivity overall and operates at peak sensitivity with wavelengths around 530 nm which corresponds excellently with the phosphor screen which phosphoresces at 545 nm. It is important to note that the phosphor camera is sensitive to 266 nm light and can be used to see the laser spot on the cathode. An example of this can be seen in Figure 17.

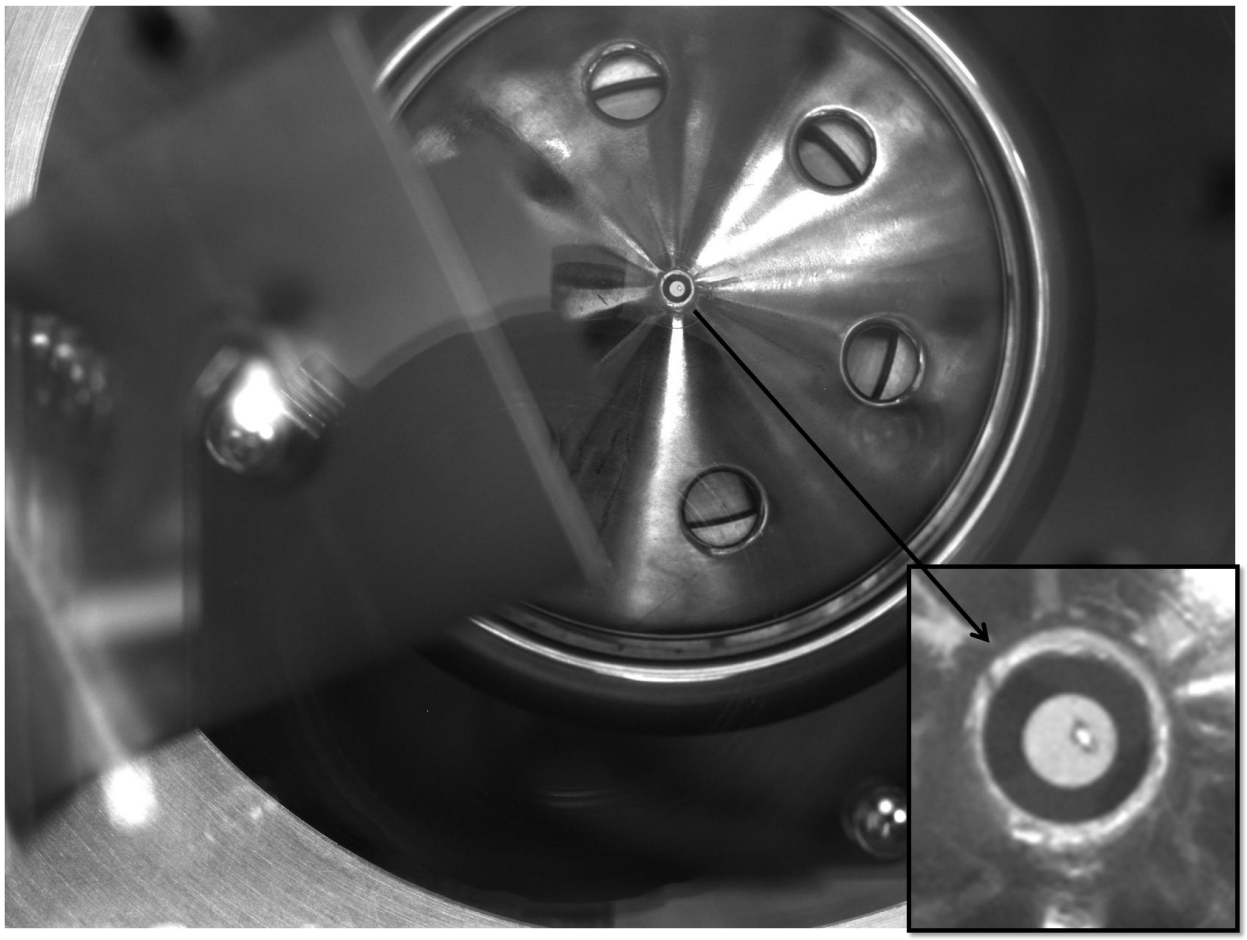

Figure 17: A picture of the Wehnelt and cathode taken using the phosphor camera from below the vacuum chamber. On the left the mirror mount and aluminum coated mirror can be seen. For this picture the anode was removed. The zoomed in image of the cathode on the lower right clearly shows the laser spot on the cathode.

The ZTEC oscilloscope has two 500 Ms/s inputs and two external trigger inputs. The input impedance can be set to 50 ohm or 1 megaohm for both input channels. It supports asynchronous capture which means the workstation can initialize capture and then continue doing other tasks (firing the laser, capturing phosphor images, etc.) while the scope waits for an external trigger to capture the samples and store them in a buffer. When the workstation is ready to initiate the next

capture, the data from the previous is waiting in the buffer and can be quickly transferred to disk over the PCI interface. Gs/s acquisition rates are achieved by internal interpolation of the A/D units in inputs 1 and 2. Thus, the workstation cannot capture data from two sources at 1Gs/s simultaneously. Instead, it alternates between capturing from channel 1 and 2 after a certain number of captured events. Each capture event consists of a cathode laser pulse and the electron cloud it produces. The system typically fires at 10 Hz.

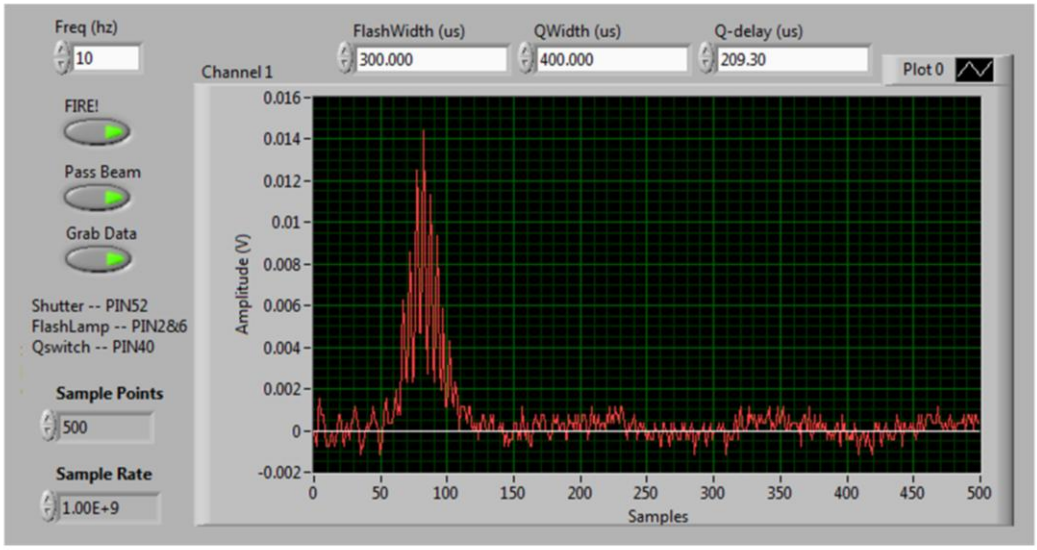

Figure 18: A screenshot of the LabVIEW front panel. A photodiode trace of a 266 nm pulse is displayed.

The data acquired from the photodiode (as seen in Figure 18) is used to characterize the temporal profile of the cathode laser. The photodiode produces current when excited by laser energy. This current creates a voltage across the 50 ohm input impedance of the scope. From the voltage trace produced by each pulse, the pulse duration as well as the temporal distribution of incident laser energy during the pulse can be backed out. The Faraday cup allows the team to characterize the electron beam in the same manner. The cup is a blackbody for electrons; every

electron which strikes the cup is absorbed and observed as current. Thus, the resulting voltages observed with the oscilloscope can be divided by the bleed resistance and integrated over the pulse duration to calculate the total number of electrons contained in each pulse. The beam sampler is outfitted with an electrical lead which provides the same data as the Faraday cup. However, the beam sampler is not a one-to-one absorber of electrons and will need to be calibrated to account for incident electrons which are not captured.

6. TEST PLAN

The test plan is not yet finalized. The goal is that the completed setup will be able to capture images of the sampled electron beam on the phosphor screen as the sampling aperture scans across the electron beam. The number of beam pulses which must be acquired at each sampling aperture location will depend on the quality of the images captured by the phosphor camera. During each beam scan, all brightness-affecting variables such as laser power, laser spot profile, anode distance, cathode voltage, Wehnelt voltage, etc. will be held constant. Once a sweep is complete, the team hopes to have an automated script to combine the phosphor camera images to create a full beam phase space profile (see Figure 19). This profile will be used to calculate the beam brightness for a given sweep. Before these calculations are possible, however, the team must complete other milestones.

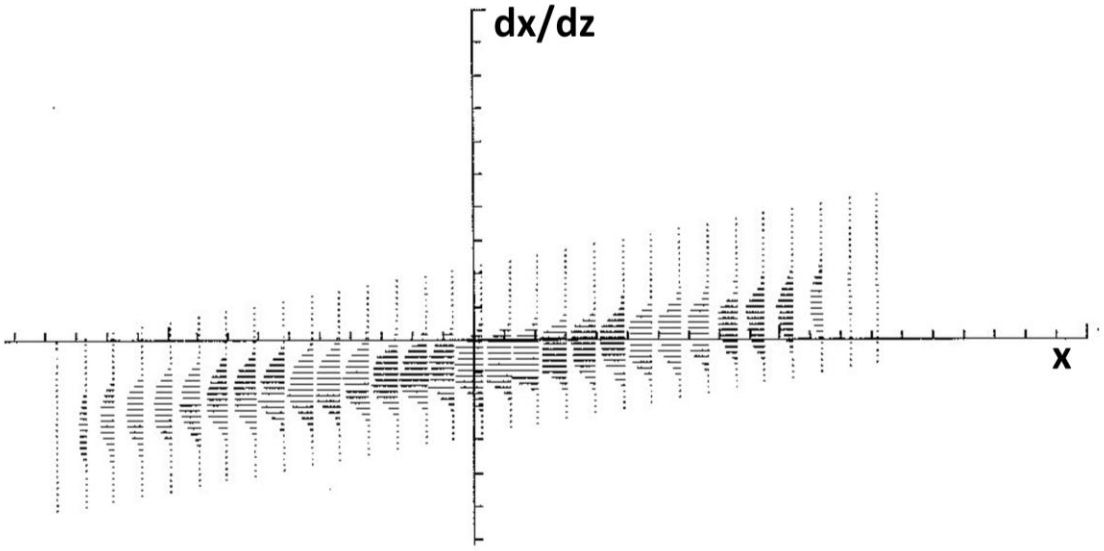

Charged Particle Beams, Stanley Humphries, 1990

Figure 19: A phase space profile for a diverging beam. The team expects to acquire data much like this once the test setup is fully functional. At each sampling aperture location *x* from the center of the beam, a distribution of the divergence of the electrons passing through the aperture is acquired with the phosphor camera.

6.1. CURRENT PROGRESS

Currently, the entire laser beam line is in place and aligned. The focused beam has been successfully passed into the vacuum chamber and focused to a spot size of fewer than 25 microns in diameter. The spot size was determined by passing the beam waist through a 25 micron aperture and measuring the power before and after the aperture. No power difference was found, indicating that the beam was passed successfully through the aperture. The photodiode and power meter have also been successfully implemented. Unfortunately, there is currently not enough power at 266 nm to use the leak-through of a mirror to produce a reading on the power

meter or photodiode. At this point, the power meter and photodiode are used to periodically check beam quality, they are not implemented as real time monitors.

The vacuum chamber has been cleaned and pumped down to below 10^{-6} torr. A mirror mount has been fabricated and placed in the vacuum chamber and the mirror has been aligned so that the laser beam is incident on the cathode. Note that the alignment is not entirely constant as the position of the cathode changes every time the electron gun is removed and replaced on the vacuum chamber. Flashes of electrons have been seen on the phosphor screen, but the team has not yet been able to obtain a static alignment that places the cathode laser beam waist on the cathode while the phosphor screen is in place.

The current procedure for placing the laser waist on the cathode using the turning mirror found in the vacuum chamber is as follows:

- With the electron gun off the chamber, form a crosshair over the center of the chamber at the desired height using a pair of thin wires.
- Using a laser viewing card and the adjustment knobs on the kinematic mount in the vacuum chamber, place waist on the crosshairs.
- Remove the wire and place the electron gun on the chamber.
- Use the phosphor camera to find the location of the spot on the electron gun.
- Remove the gun and adjust the beam location as necessary.
- Repeat the previous two steps until the spot is centered on the cathode.
- Seal the chamber and pump down.
- If the spot remains on the cathode, the system is aligned.

As the phosphor screen can be moved around the chamber while sealed and at vacuum (using a strong magnet outside the chamber and a ring of steel around the phosphor screen), a large degree of uncertainty in the alignment has been removed as the electron gun no longer needs to be removed to move the phosphor screen in place (at the same time blocking the phosphor camera, making a check on the alignment impossible). However, as the position of the cathode/Wehnelt changes by approximately 200 microns every time the electron gun is placed on the chamber, it is almost impossible to successfully and consistently place the laser spot on the cathode. In the future work section, a new alignment procedure is explained.

The phosphor camera has been integrated into the setup and takes exposures containing anywhere from 5 to over 100 pulses depending on the time needed to get good images of the phosphorescence. The camera can be configured to acquire short exposures centered in time around each electron pulse (this drastically decreases the effect of ambient light), but the synchronization between the laser trigger and camera trigger is not sufficiently precise to produce reliable results using this method. This lack of precision stems from a quirk in the triggering support within the camera's LabVIEW drivers. For now, the team has settled on pairing the long exposure method with a skirt of blackout cloth around the base of the vacuum chamber to block out ambient light.

6.2. FUTURE WORK

The motor-actuated linear translation feed-through needs to be placed on the vacuum chamber and verified that it holds vacuum better than 10^{-6} torr. The Faraday cup and the knife edge also need to be cleaned and placed into the chamber. Once they are placed inside the chamber, the beam measurement devices need to be calibrated.

Calibration of the electron beam measurement equipment will require cross-calibration between charge collected in the Faraday cup, charge collected on the beam sampler, and the brightness of phosphorescence on the phosphor screen. The one-to-one Faraday cup will be used as a reference (as current entering the cup is caught), but since all three measurement techniques sample different sized portions of the non-uniform electron beam, reconciling their results will be non-trivial. This will be done once the team can reliably align the laser waist on the cathode and are able to produce electrons (verified with phosphorescence from the phosphor screen).

Depending on the amount of brightness data which the team is able to collect before the end of the school year, different analysis techniques will be used. Limited to varying a single variable (laser spot size for example), the team will provide basic relationships between that variable and the brightness of the electron beam. In addition to brightness, other potentially interesting metrics will be included since it is important to know how a certain change in the system increases or decreases the electron beam brightness. These metrics include the total beam current, the beam spatial intensity pattern, and the beam's local convergence distribution. Characterizing additional measurements, such as the symmetry of the electron beam, may also be

informative. If this data is accumulated for a wide range of inputs (laser power, laser spot profile, anode distance, cathode voltage, Wehnelt voltage, etc.), then the team will be able to fit a multivariable model to the data, providing predictions of various electron beam characteristics as a function of these inputs.

A new alignment procedure also needs to be tested and possibly refined. In order to correct for the uncertainty in position of the cathode/Wehnelt when placing the electron gun on the chamber, the following procedure should be used:

- With the electron gun off the chamber, form a crosshair over the center of the chamber at the desired height using a pair of thin wires.
- Using a laser viewing card and the adjustment knobs on the kinematic mount in the vacuum chamber, place waist on the crosshairs.
- Remove the wire and place the electron gun on the chamber.
- Use the phosphor camera to ensure that the spot is reasonably close to the cathode.
- Seal the chamber and pump down. This is to check that the electron gun is properly placed and tightened on the chamber.
- Return to atmospheric pressure and remove the bottom window of the vacuum chamber.
- Using the adjustment knobs on the kinematic mount in the vacuum chamber, place the spot on the cathode.
- Replace the bottom of the chamber.
    - Do not forget to place the phosphor screen in the chamber before sealing the bottom.
- Seal the chamber and pump down.

- If the spot remains centered on the cathode, the system is aligned.

The team has an old thermocouple gauge to use as a vacuum interlock; however, the comparator circuit to trigger a switch if the chamber vacuum rises to above 1e-4 Torr (as described in section 5) has not yet been assembled. The interlock will prevent voltage breakdown from occurring between the Wehnelt at -33 kV and the anode at ground (located approximately 1 cm from the Wehnelt). Until the interlock is complete, the team will operate at reduced voltage. Tests with a Geiger counter show no detectable quantity of radiation escaping the chamber when breakdown occurs at 24 kV.

7. REFERENCES

Born, Max, and Emil Wolf. Principles of Optics; Electromagnetic Theory of Propagation, Interference and Diffraction of Light,. Oxford: Pergamon, 1970

Hecht, Eugene, and Alfred Zajac. *Optics*. Reading, MA: Addison-Wesley Pub., 2002.

Humphries, Stanley. "Introduction to Beam Emittance." *Charged Particle Beams*. New York: Wiley, 1990.

Jenkins, Francis A., and Harvey Elliott White. *Fundamentals of Optics*. New York: McGraw-Hill, 1957.

Michael R. Armstrong, et. al, "Practical Considerations for High Spatial and Temporal Resolution Dynamic Transmission Electron Microscopy." *Ultramicroscopy* 107 (2007): 356-367.

Lawrence Livermore National Laboratory (LLNL): What We Do . Lawrence-Livermore National Laboratory. 20 Sept. 2010 < https://www.llnl.gov/about/whatwedo.html>.

Reed, Bryan W., et. al, “Nanosecond Dynamic Transmission Electron Microscopy.” PowerPoint presentation. 9 Sept. 2010.

Reed, Bryan W., et. al, "The Evolution of Ultrafast Electron Microscope Instrumentation." *Microscopy and Microanalysis* 15 (2009): 272-81.

Schamber, Fred, et. al., "Emission Myths." *Microscopy Today* (1999): 1-10.

Worster, J., "The Brightness of Electron Beams." *British Journal of Applied Physics* 2nd ser. 2 (1969): 457-62.

Appendix A – System Operation

This is intended as a guide to turning on the full test bed. This is meant as a routine operation procedure, for the initial start up of the Spectra-Physics GCR 190 laser and the Alcatel pumping station, please consult the respective manuals. Portions of this procedure can be omitted depending on the tasks being performed.

- Turn on the computer and access the full system VI and the GigE camera viewer.
- Turn on the dry nitrogen flow, with a 2 stage regulator, the output pressure should read around 20 psi with the output valve slightly open.
- Remove the desiccant jar (taking care not to disturb the alignment of the crystal).
- Position the nitrogen hose so there is a constant flow on the face of the crystal.
- Turn up the lamp energy on the laser to 10 and start the laser firing using the VI.
- Check the alignment of the laser spot in the cathode using the camera.
- If it good, check the chamber to make sure it is sealed and pump it down. You can also drag the phosphor screen in place at this time.
- After the laser has reached thermal equilibrium and is stable, check the beam quality and power using the photodiode and power meter
- Once the chamber is pumped down past 10^{-5} torr, connect the HV leads and turn on the power supply, checking to make sure the interlock is working.
- When the chamber is around/below 5e-6 torr, the voltage can be turned up.
    - Turn up the voltage slowly and check to make sure there is no breakdown/accidental path to ground.
- The system is now on and ready for data acquisition.

Appendix B – VI Operation

The LabVIEW front panel display has been reproduced in Figure 20.

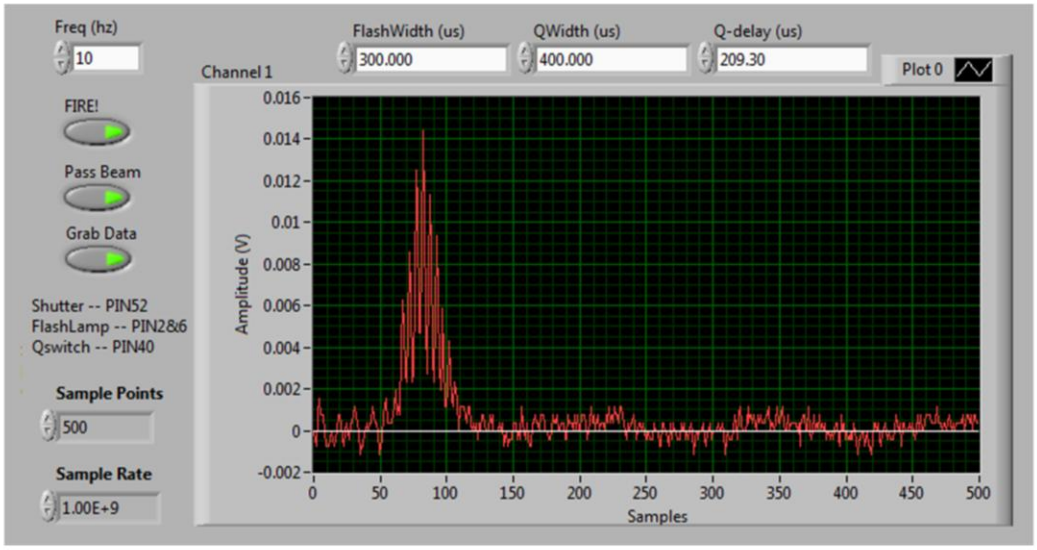

Figure 20: LabVIEW front panel.

The VI is designed to send trigger outputs to the laser and shutter system, as well as collect data through the two channels in the system oscilloscope.

- Frequency of the laser and shutter system can be modified in the top left corner of the VI, provided that the frequency is within operational specifications of the laser unit.
- The "FIRE!" button determines if the laser is firing or not, whiles the shutter operates if the "Pass Beam" button has been activated.
- Specifications of the laser, such as flash width, Q-switch width, and Q-switch delay, can be modified above the graph in the VI.
- The oscilloscope can be told to obtain data using the "Grab Data" function. The number of samples and the sample rate can be modified below the button.

Appendix C – Team Member Profiles

Perry Ellis is a senior physics major at Harvey Mudd College. Last spring, he studied abroad in Granada, Spain enjoying the finer side of life. After returning, he spent the summer at Harvey Mudd College characterizing and researching the binding of antibodies to gold nanospheres. After graduation, Perry plans to pursue a Ph.D. in physics at Georgia Tech. Apart from academics, Perry enjoys rock climbing, playing waterpolo, and daydreaming about Spain.

Zeke Flom is a senior engineering major at Harvey Mudd College who still doesn't know what he wants to be when he grows up. He interned at Raytheon's Space and Airborne Systems last summer where he gained experience with RF design, simulation, testing, and troubleshooting. Zeke is planning to work for some time before returning to school to pursue a Ph.D. in electrical engineering, robotics, or whatever strikes his fancy. In his free time he loves to play soccer, freeline, listen to music, and build things.

Tim Nguyen is a senior engineering major at Harvey Mudd College, interested primarily in control theory and embedded systems. Tim has taken electives in VLSI CMOS design and is currently enrolled in electives in Control Systems and Microprocessor Systems. He interned at Cardinal Peak last summer, working on signal processing analysis of electronics for patent infringement cases and on the design (primarily coding) of a prototype testbench. Tim is considering eventually pursuing a Ph.D. in control theory or an MBA after graduation. His other interests include music, cycling, card games, and tinkering with things.

Spencer Tung is a junior engineering major at Harvey Mudd College. He has taken courses in both mechanical and electrical engineering. He held a research position with the Engman Fellowship last summer, studying the stiffness of nasal tip cartilage with a fellow researcher. After graduation, he intends to find a job in electrical engineering for a few years before

returning to graduate school to pursue an MS or Ph.D. His other interests include ballroom dance, voice, and relaxing with friends.

Karen Heinselman is a junior engineering major at Harvey Mudd College. Karen has taken Physical Chemistry and is currently enrolled in the Engineering Electronics elective. She spent last summer doing research at Harvey Mudd College on binary phase diagrams of eco-friendly surfactants, and has spent a summer (2009) at SRI International researching upper-atmospheric chemistry. She is considering pursuing a Ph.D or MBA after graduation. Karen is interested in chemical, materials and electrical engineering. Her other interests include ballroom dancing, music, reading, and longboarding in heels.